Lin *et al.*
Chinese Journal of Mechanical Engineering (2023) 36:133
https://doi.org/10.1186/s10033-023-00959-6

Chinese Journal of Mechanical Engineering

ORIGINAL ARTICLE

Open Access

Well-Dispersed Graphene Enhanced Lithium Complex Grease Toward High-Efficient Lubrication

Kaiyue Lin[1], Zhuang Zhao[1], Yuting Li[1], Zihan Zeng[1], Xiaofeng Wei[1], Xiaoqiang Fan[1*] and Minhao Zhu[1,2*]

Abstract

Graphene as a lubricating additive holds great potential for industrial lubrication. However, its poor dispersity and compatibility with base oils and grease hinder maximizing performance. Here, the influence of graphene dispersion on the thickening effect and lubrication function is considered. A well-dispersed lubricant additive was obtained via trihexyl tetradecyl phosphonium bis(2-ethylhexyl) phosphate modified graphene ([P_{66614}][DEHP]-G). Then lithium complex grease was prepared by saponification with 12-OH stearic acid, sebacic acid, and lithium hydroxide, using polyalphaolefin (PAO20) as base oil and the modified-graphene as lubricating additive, with the original graphene as a comparison. The physicochemical properties and lubrication performance of the as-prepared greases were evaluated in detail. The results show that the as-prepared greases have high dropping point and colloidal stability. Furthermore, modified-graphene lithium complex grease offered the best friction reduction and anti-wear abilities, manifesting the reduction of friction coefficient and wear volume up to 18.84% and 67.34%, respectively. With base oil overflow and afflux, well-dispersed [P_{66614}][DEHP]-G was readily adsorbed to the worn surfaces, resulting in the formation of a continuous and dense graphene deposition film. The synergy of deposited graphene-film, spilled oil, and adhesive grease greatly improves the lubrication function of grease. This research paves the way for modulating high-performance lithium complex grease to reduce the friction and wear of movable machinery.

Keywords Graphene additive, Lithium complex grease, Dispersion, Tribological properties

1 Introduction

Grease with excellent lubrication properties is effective in improving the friction and wear of movable equipment components to a certain extent, avoiding mechanical component failure and safety problems as a common semi-solid lubricant for bearings, gears, and chain components [1, 2]. In addition, it has the unique advantages of great sealing, high water resistance, and strong adhesion, can adhere to the friction substrate under gravity, and prevents impurities or rainwater from entering the worn surface [3, 4]. Grease is mainly composed of base oil, thickener, and additives [5]. Base oil and thickener account for about 70% to 98% and 2% to 30% of grease, respectively. The thickener forms a three-dimensional space skeleton structure in the base oil, which can adsorb and fix the base oil [6]. Base oil and thickener play a decisive role in the high temperature resistance, colloidal stability, and rheology of lubricating grease [7–9]. Currently, lithium complex grease is typically a general-purpose grease with high dropping point and versatility. With the rapid development of industry, mechanical equipment inevitably faces the

*Correspondence:
Xiaoqiang Fan
fxq@home.swjtu.edu.cn
Minhao Zhu
zhuminhao@home.swjtu.edu.cn
[1] Key Laboratory of Advanced Technologies of Materials (Ministry of Education), School of Materials Science and Engineering, Southwest Jiaotong University, Chengdu 610031, China
[2] Tribology Research Institute, School of Mechanical Engineering, Southwest Jiaotong University, Chengdu 610031, China

severe impact of harsh and extreme working environments, such as heavy loads, vibration, shock, sandstorms, heavy rain, high or low temperatures and speeds, and so forth [10–13]. The traditional lithium complex grease no longer meets the demands of industrial machinery and equipment for better performance. A common way to enhance the lubricating properties is to introduce additives into the grease, such as copper oxide nanoparticles (CuO) [14, 15], nano-particles (TiO_2/CuO) [16], $CaCO_3$ nanoparticles [17], nanometer cerium oxide (CeO_2) [18], nano-additives ($CaCO_3$) [19], TiO_2 nanoparticles [20], Mn_3O_4/graphene nanocomposite [21], graphene [22], graphene-copper nanocomposite [23], etc. Among them, two-dimensional materials, in particular graphene and its derivatives, are widely used in the field of lubrication.

Graphene is a promising grease additive with excellent thermal conductivity, high mechanical strength, a high specific surface area, and low shear strength [24–27]. In recent years, many researchers have reported on the effects of graphene as a grease additive. Li et al. [28] investigated the tribological properties of lithium greases with few-layer graphene (FLG) and found that the lithium greases containing 0.1 wt% FLG exhibited the lowest friction coefficient and the smallest wear scar diameter. This is attributed to the fact that it is easy to adsorb on the contact interface due to the high specific surface area. Additionally, when subjected to external forces, graphene is prone to interlayer shearing due to weak Van der Waals connections. Ouyang et al. [29] introduced 3D hierarchical porous graphene (3D HPGS) into a lithium-based grease and conducted friction tests on friction testers with different contact modes (four-ball tribometer, rotating tribometer, reciprocating tribometer) and came to the similar conclusion that graphene could improve the tribological properties of the grease. Rawat et al. [30] found that the addition of pristine graphene significantly improved the tribological properties of the paraffin grease. The authors believe that the graphene film formed protects the worn surface and reduces wear. These studies confirmed that graphene can be used as a promising grease additive. However, the unresolved problem is that graphene tends to agglomerate and sediment in the base oil due to the strong attractive force between graphene sheets, which affects the lubrication effect of grease [31].

Currently, graphene-like materials can be functionalized by grafting surfactants or in situ growth of nanomaterials on the surface of graphene-like materials [32, 33]. A series of functionalized graphenes, such as curcumin modified graphene oxide (C-GO) [34], dodecylamine functionalized graphene (DAG) [35], 3,5-di-tert-butyl-4-hydroxybenzaldehyde grafted-graphene (Gr-DtBHBA) [36] and graphene oxide-TiO_2 nanofluid [33] exhibit good compatibility in oils or solvents, which helps to avoid the dispersibility of graphene base oils to some extent. However, these functionalized graphenes might find it difficult to survive some harsh friction conditions due to limited thermal stability and lubrication properties at 100 °C. Hence, it is essential to investigate graphene base oils with excellent thermal stability and lubrication properties at high temperatures. Gan et al. [37] investigated the lubricating properties of phosphonium-organophosphorus modified graphene in 150 N base oil and proposed a simple method to prepare functionalized graphene lubricants. The results showed that the modified graphene was completely and stably dispersed in 150 N oil. The modified graphene used as a lubricant showed a narrow and shallow wear track with minimal wear debris. The modified graphene base oil shows excellent thermal stability and tribological properties at high temperatures and high loads, so it could be used in harsh conditions. However, the lubrication mechanism of phosphonium-organophosphate modified graphene as a grease additive remains unclear due to the presence of thickener fiber in the grease. Motivated by this, we attempted to add phosphonium-organophosphate modified graphene to polyalphaolefin oil (PAO20) and prepared graphene grease in a one-step process using a modified-graphene base oil with good dispersibility. Well-dispersed graphene was compounded in situ with thickener fiber in the formation process. The tribological performance of modified-graphene greases under different working conditions, high loads, and durations was investigated. Most of the current research on the lubrication performance of graphene greases focuses on frictional interfacial phenomena while ignoring the fact that the dispersion stability of graphene in the base oil may lead to changes in the thickener fiber. Indeed, so far, few studies have investigated the relationship between the dispersibility of graphene and the lubrication mechanism of greases. The formation and distribution of graphene deposition films could be revealed by Raman spectroscopy. Graphene greases with good dispersion provide better lubricity than the original graphene grease.

In this paper, graphene with good dispersion was prepared by using trihexyl tetradecyl phosphonium bis(2-ethylhexyl) phosphate as an oil-soluble modifier, with original graphene as a comparison. The lithium complex grease was prepared via a facile one-step method. The morphology and structure of graphene were systematically studied by transmission electron microscopy, atomic force microscopy, and Raman spectroscopy. Moreover, the physicochemical properties of graphene lithium complex grease and tribological performance at high and low loads were explored. The worn surface was

observed by a scanning electron microscope and white light interferometer, and the lubrication mechanism of graphene grease was proposed.

2 Experimental Details

2.1 Materials

Graphene (G) was purchased from Suzhou Carbon Abundant Graphene Technology Co. Ltd. (Suzhou, China). Sebacic acid, 12-OH stearic acid, lithium hydroxide (LiOH), hexane, and sodium hydroxide (NaOH) were supplied from Kelong Chemical Co. Ltd. (Chengdu, China). Base oil (PAO20) was supplied by Lanzhou Refining Co. (Lanzhou, China). Tetradecyl trihexyl phosphonium bromide ([P66614]Br) and bis(2-ethylhexyl) phosphate (HDEHP) were obtained by Hubei Yongkuo Technology Co. Ltd. Deionized water (DIW) was provided by the laboratory (>18 MΩ·cm).

2.2 Preparation of Graphene Lithium Complex Grease

In this experiment, graphene lithium complex grease with a thickener content of 12% was prepared with PAO20 as base oil. Three kinds of base oils, namely pure base oil, base oil containing pristine graphene, and base oil containing modified-graphene, were used to respectively fabricate three types of greases, namely lithium complex grease (LCG), graphene lithium complex grease (G-LCG), and modified-graphene lithium complex grease ([P_{66614}][DEHP]-G-LCG). Figure 1 shows the digital images of three different greases. The graphene base oil was prepared by adding 0.1 wt% of pristine graphene or modified-graphene to the base oil and ultrasonicating for 30 min to assure homogeneous dispersion.

The preparation process for grease is described as follows: 66 g base oil was heated up to 120 °C, accompanied by mechanical stirring, and 9.455 g 12-OH stearic acid and 2.545 g sebacic acid (1:0.4 molar ration) were added successively in base oil and dissolved completely to obtain the mixture. Then, 3.166 g LiOH was dissolved in 10 ml DIW, and LiOH aqueous solution was slowly added to the mixture for about 20 min. The saponification reaction was carried out at 115 °C for 1 h. Next, 22 g base oil was added to the mixture and stirred evenly. The temperature of the mixture was raised to 205 °C for high-temperature refining and held for 10 min. Finally, the mixture was removed and cooled to room temperature. The grease was obtained by grounding or homogenizing the mixture four times on a three-roll mill. Graphene ([P_{66614}][DEHP]-G) modified by trihexyl tetradecyl phosphonium phosphate bis (2-ethylhexyl) was prepared according to the reference [37]. The detailed steps are demonstrated as follows: 8.96 g [P_{66614}]Br, 51.3 g HDEHP, 40 ml DIW and 25 ml hexane were added sequentially to the beaker, accompanied by magnetic stirring, and the yellow organic phase changed to colorless at the end of the reaction. Then, 0.64 g NaOH was added to the above solution under magnetic stirring (4 h) to remove the reaction by-product (HBr). The organic phase trihexyl tetradecyl phosphonium bis (2-ethylhexyl) phosphate ([P_{66614}][DEHP]) was separated from the solution by centrifugation at 7000 r/min for 6 min, prior to being washed five times with DIW to ensure the removal of NaBr. [P_{66614}][DEHP] was dried in a vacuum drying oven at 80 °C for 12 h to remove excess water and hexane. Finally, [P_{66614}][DEHP]-G was obtained via grinding an appropriate amount of [P_{66614}][DEHP] and pristine graphene.

2.3 Physicochemical Properties of Grease

The dropping point of greases was evaluated by a drop point tester according to ASTM-D566 at an ambient temperature of 25 °C with a nominal voltage of 220 V and a frequency of 50 Hz. The cone penetration was measured by the lubricating grease cone penetration instrument following the national standard GB/T 269 (ASTM D1403), which represented the consistency of the grease. The cup of the appropriate grease worker was tightly filled with grease. The cone assembly of the device was released, and the cone was allowed to fall freely into the worker cup for 5 ± 0.1 s. The three test results were

Figure 1 Representative photos of prepared grease: (**a**) LCG, (**b**) G-LCG, and (**c**) [P_{66614}][DEHP]-G-LCG

averaged as the reported result. The corrosion resistance of copper strips to grease was measured based on the national standard GB/T 7326-87 (ASTM D4048-81). The surface of the copper strip was coated with grease, and then the sample was put into a circulating air oven at 100 ± 1 °C for 24 h ± 5 min. At the end of the test, the strip was washed and compared with the Copper Strip Corrosion Standard to detect the corrosion of the copper strip. The oil separation test was performed by loading a 10 g sample into the stencil and measuring the colloidal stability of grease at 100 °C for 30 h according to the national petrochemical industry standard NB/SH/T 0324-92.

2.4 Tribological Properties of As-Prepared Grease

The tribological properties of the as-prepared grease under low load and high load were respectively evaluated by the reciprocating sliding friction tester and the four-ball friction tester. The tribological properties of grease under low loads were determined by reciprocating sliding friction tests. The ball-on-disk configuration was adopted. The AISI 52100 steel ball with a diameter of 6 mm and a surface roughness of Ra = 50 nm and the AISI 52100 steel blocks with a surface roughness of Ra = 80 nm were used as the counter ball and the substrate, respectively. The test parameters were as follows: displacement amplitude of 4 mm, normal loads of 20 N, 40 N, and 60 N, and testing time of 60 min. In the process of the reciprocating sliding friction test, the friction coefficient was measured and recorded automatically by the computer. The friction test under high loads was carried out with a four-ball friction tester. 8 g lubricating grease was injected into the oil cup so that the contact area of the steel ball was completely covered with grease. The four-ball friction tests were measured at a rotational speed of 1200 revolutions per minute (r/min) with an applied force of 392 N and 490 N for 1 h. Both upper and lower steel balls were standard AISI 52100 bearing steel with a diameter of 12.7 mm and a surface roughness of Ra = 20 nm. The wear scar diameters of the steel balls were measured with an optical microscope on the four-ball tester and then averaged. Besides, all friction pairs were ultrasonically cleaned with ethanol or petroleum ether three times for 20 min before the friction test, and the residual grease on the worn surface was removed with petroleum and alcohol after each friction test. The same friction tests were repeated three times under the same operating conditions to ensure the accuracy and repeatability of the test results.

2.5 Characterization of Graphene and Worn Surface

The morphology and characteristics of graphene were studied by transmission electron microscopy (TEM, JEM-2100F, Japan), atomic force microscopy (AFM, FM-Nanoview1000), and Raman spectroscopy (Raman, LabRam HR800, Japan). The functional groups of the graphene were measured by Fourier transform infrared spectroscopy (FTIR, Nicolet-6700, America). The wear volume, worn surface morphology, and wear mechanism of the friction interface were characterized using a white light interferometer (Bruker Contour GT), a scanning electron microscope (SEM, JSM-7800F, Japan), and Raman spectroscopy.

3 Results and Discussion

3.1 Physicochemical Properties

The physicochemical properties of as-prepared greases are summarized in Table 1. The results show excellent thermal stability of [P_{66614}][DEHP]-G-LCG, and the dropping points of as-prepared greases are all greater than 230 °C. In the copper corrosion test, there was no change in the color of the copper strip, and the copper strip corrosion grades are all 1a, ensuring that the as-prepared greases possess superior corrosion resistance to protect the metal surfaces. The oil separation test results reveal that the colloidal stability is improved in the following order: G-LCG < LCG < [P_{66614}][DEHP]-G-LCG, and the oil separation is less than 10% in all cases, indicating the good colloidal stability of as-prepared grease [38].

3.2 Characterization of G and [P_{66614}][DEHP]-G

The TEM images of G and [P_{66614}][DEHP]-G and atomic force images of G are shown in Figure 2. G has a characteristic two-dimensional lamellar structure with folding phenomena. [P_{66614}][DEHP]-G also presents a complete two-dimensional sheet structure in Figures 2b. It means

Table 1 Physicochemical properties of as-prepared greases

Project	Dropping point (°C)	Penetration (1/4 mm)	Copper corrosion (100 °C, 24 h)	Oil separation (%)
Detection standards	ASTM-D566	ASTM-D217	ASTM-D4048-81	SH/T 0324-92
LCG	235	92.84	1a	2.46
G-LCG	241	96.12	1a	2.17
[P_{66614}][DEHP]-G-LCG	238	97.14	1a	3.56

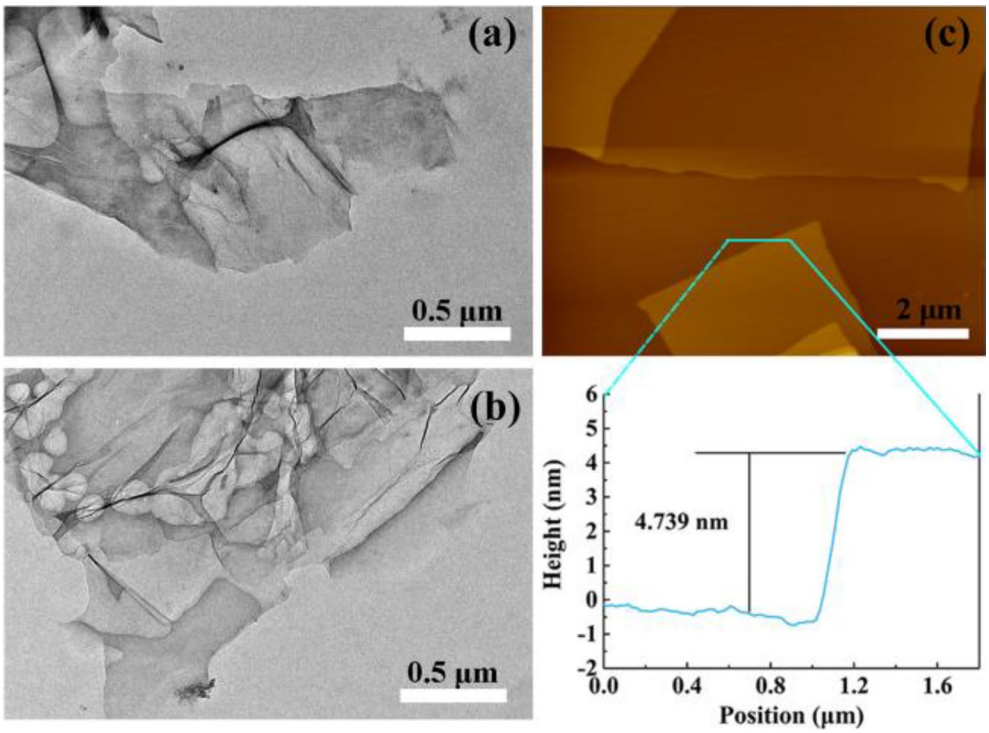

Figure 2 TEM images of (**a**) G and (**b**) [P_{66614}][DEHP]-G, (**c**) AFM images and corresponding height maps

that the layered structure of modified-graphene nearly is not damaged. The size of G flakes measured by AFM is 4.739 nm. It is widely believed that the theoretical thickness of single-layer graphene is 0.335 nm. In practical measurements, the thickness of a single-layer graphene is approximately 0.9 nm due to the additional space between graphene and mica sheet [39, 40].

Figures 3(a) and (b) show the Raman spectra of G and [P_{66614}][DEHP]-G. The peak positions of G and [P_{66614}][DEHP]-G in the D and G bands are consistent. The D band of graphene emerges at 1334 cm^{-1}, which is a disordered vibration peak due to lattice vibration, indicating the presence of edge and structural defects [41]. G band appears at 1573 cm^{-1}. The main characteristic peak of G band is caused by the in-plane vibration of sp^2 carbon atoms [42]. The degree of defects and disorder in graphene can be measured by the intensity ratio of the D band to the G band (I_D/I_G), which increases with the value of I_D/I_G [43]. Compared to G (I_D/I_G:1.41), the I_D/I_G value of [P_{66614}][DEHP]-G is lower (0.88), demonstrating [P_{66614}][DEHP]-G has a smaller defect density and degree of disorder [44]. Figures 3c and d display the functional groups of G and [P_{66614}][DEHP]-G measured by FTIR spectra. In the spectrum of G, the peak at 3438 cm^{-1} corresponds to the O–H stretching vibration and that at 1633 cm^{-1} to the stretching vibration of the C=C bond. The FTIR spectra of [P_{66614}][DEHP]-G shows characteristic peaks at 2852 cm^{-1}, 2871 cm^{-1}, 2929 cm^{-1} and 2954 cm^{-1}, which are attributed to the C–H stretching vibration. The peak at 1238 cm^{-1} corresponds to the P=O stretching vibration of [P_{66614}][DEHP]-G. Additionally, the P–O–C absorption peaks appeared at 1041 cm^{-1} and 1056 cm^{-1} [45]. The existence of these linkages demonstrates that [P_{66614}] [DEHP] is indeed adsorbed on graphene sheets.

To assess the dispersion stability of [P_{66614}][DEHP]-G in base oil, G and [P_{66614}][DEHP]-G were homogeneously dispersed in base oil by sonication (concentration of 0.1 wt%). The dispersion of G and [P_{66614}][DEHP]-G base oils standing at room temperature for 0 and 30 days is depicted in Figure 4. G in base oil gradually agglomerated and settled, with obvious stratification after standing for 30 days. In contrast, [P_{66614}][DEHP]-G still remained well dispersed after resting for 30 days, showing good dispersion stability. More importantly, the dispersion homogeneity and stability of graphene affect the tribological properties of as-prepared greases.

3.3 Tribological Properties of Lubricating Grease

Friction and wear behaviors of graphene lithium complex greases under low loads are examined on a reciprocating sliding friction test machine. Figures 5(a), (c), and (e) show time-dependent friction coefficients of LCG, G-LCG, and [P_{66614}][DEHP]-G-LCG at 20 N, 40

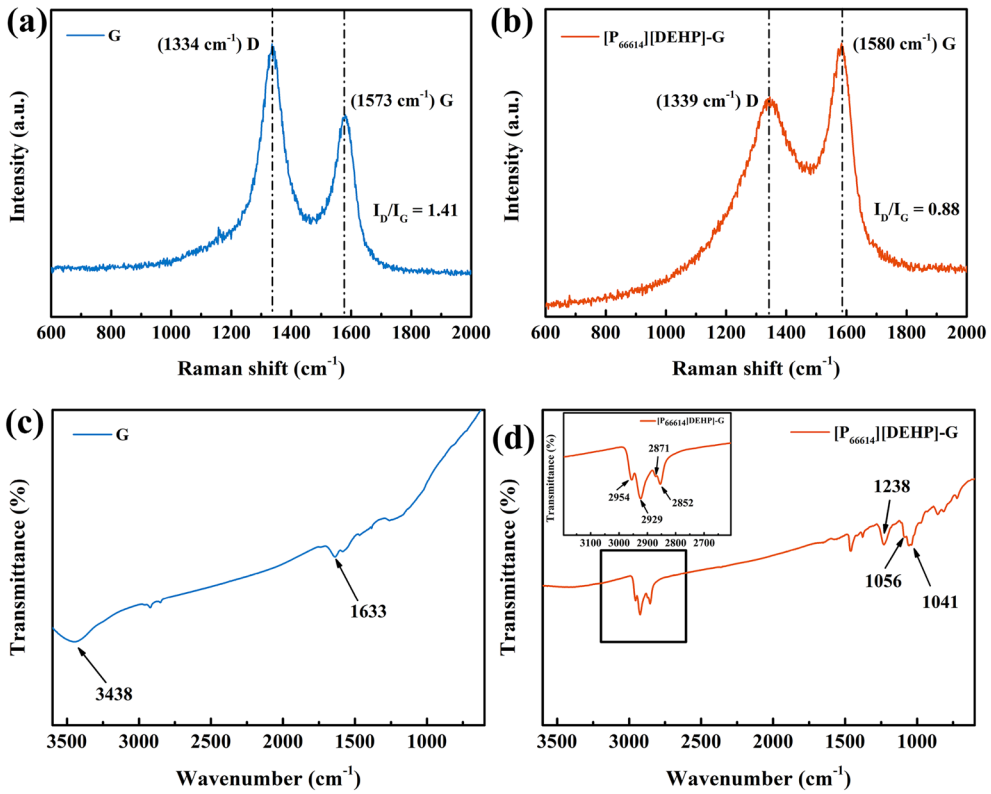

Figure 3 Raman (**a**, **b**) and FTIR (**c**, **d**) spectra of G and [P_{66614}][DEHP]-G

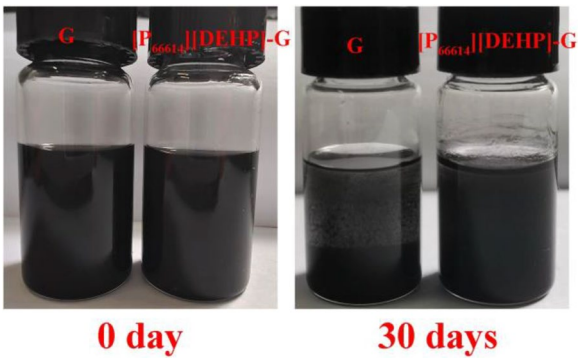

Figure 4 Optical images of G and [P_{66614}][DEHP]-G dispersing in base oil as a function of time (from 0 day to 30 days)

N, and 60 N, respectively. Under all loading conditions, lithium complex grease exhibits a higher friction coefficient (with the increase in load, the friction coefficient is in the range of 0.100-0.115). However, the friction coefficients of G-LCG and [P_{66614}][DEHP]-G-LCG are lower than those of LCG under all loading conditions and were relatively stable. [P_{66614}][DEHP]-G-LCG shows the lowest coefficient of friction (in the range of 0.085–0.093). In particular, [P_{66614}][DEHP]-G-LCG shows excellent friction reduction in the steady state stage at 60 N, with a friction coefficient reduction of 18.84%. Figures 5(b), (d), and (f) exhibit the wear volumes of LCG, G-LCG, and [P_{66614}][DEHP]-G-LCG at different applied loads (20 N, 40 N, and 60 N), where the wear volumes of G-LCG and [P_{66614}][DEHP]-G-LCG decreased compared to those of LCG. Most importantly, [P_{66614}][DEHP]-G-LCG demonstrates the most excellent anti-wear characteristic. The wear volumes of G-LCG and [P_{66614}][DEHP]-G-LCG were reduced by 56.88% and 67.34% at 60 N, respectively. The aforementioned evidence indicates that G and [P_{66614}][DEHP]-G may access friction contact and participate in the friction process, resulting in a low friction coefficient. The well-dispersed [P_{66614}][DEHP]-G demonstrates superior anti-friction and anti-wear capabilities, which may be attributable to the creation of a dense lubricating film, improving the lubricating performance of grease. superior anti-friction and anti-wear capabilities, which may be attributable to the creation of a dense lubricating film, improving the lubricating performance of grease.

In order to further explore the friction performance of graphene lithium complex grease, the four-ball test machine was used for the friction test. Figure 6 shows the coefficient of friction, wear scar diameter (WSD), and

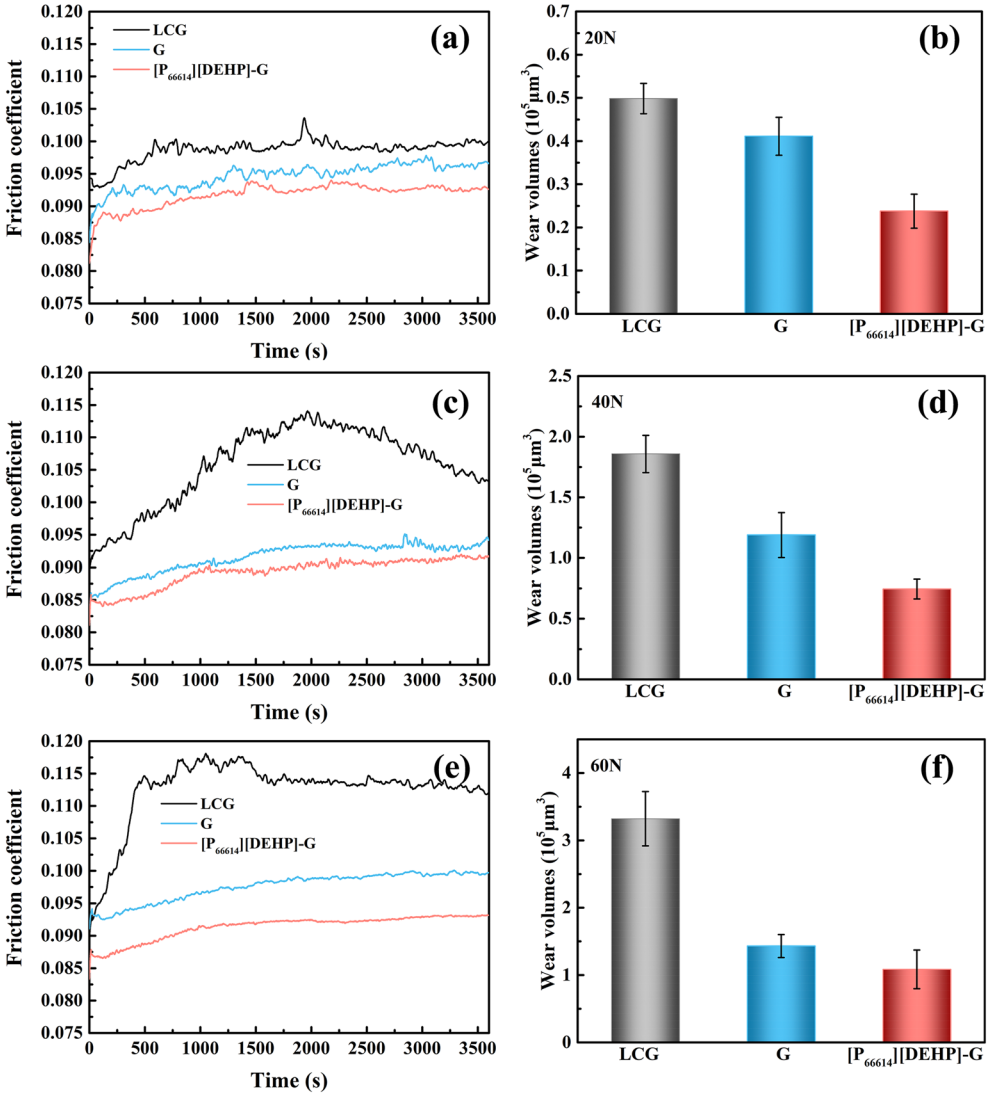

Figure 5 Friction coefficients and wear volumes of as-prepared grease at (**a**, **b**) 20 N, (**c**, **d**) 40 N, and (**e**, **f**) 60 N

average friction coefficient (AFC) of the three greases on a four-ball friction tester at 392 N and 490 N. As shown in Figures 6a and b, [P_{66614}][DEHP]-G-LCG shows the lowest friction coefficient compared with the frictional behaviors of LCG and G-LCG. Figure 6d exhibits the average friction coefficient on steel balls. With the addition of [P_{66614}][DEHP]-G, the friction coefficient was averagely reduced to 0.066 (decreased by 22.4% compared with LCG), demonstrating that [P_{66614}][DEHP]-G offers good anti-friction ability under high loads. [P_{66614}][DEHP]-G-LCG presented the best anti-wear properties (12.3% reduction in wear scar diameter) at 392 N. At 490 N, the [P_{66614}][DEHP]-G-LCG shows the smallest wear scar diameter. Both graphene lithium complex greases exhibit better anti-wear properties than LCG under high loads. [P_{66614}][DEHP]-G-LCG displays the most excellent anti-wear properties under different operating conditions, which was potentially attributed to the adsorption of graphene on the friction interface, reducing the resistance between the friction pairs and friction and wear. Notably, friction test results under high loads are consistent with the anti-friction and anti-wear effects of sliding friction tests.

The state of worn surfaces was further explored by describing the 3D morphologies and cross-sectional profiles of steel balls after a standard four-ball friction test (Figure 7). As demonstrated in the 2D contour plots, the cross-sectional contour plots for the [P_{66614}][DEHP]-G-LCG exhibit the smallest wear scar width and shallowest wear depth. Figure 8 shows the

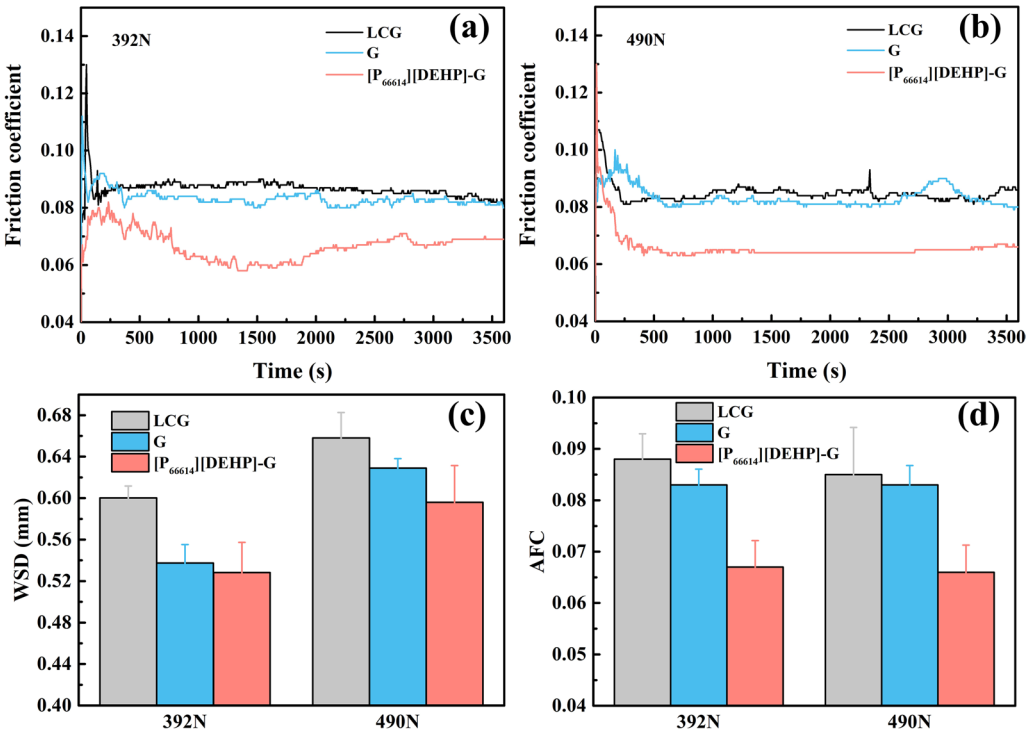

Figure 6 The friction coefficient, corresponding wear scar diameter (WSD), and average friction coefficient (AFC) of as-prepared grease on a four-ball testing machine with loads of 392 N and 490 N

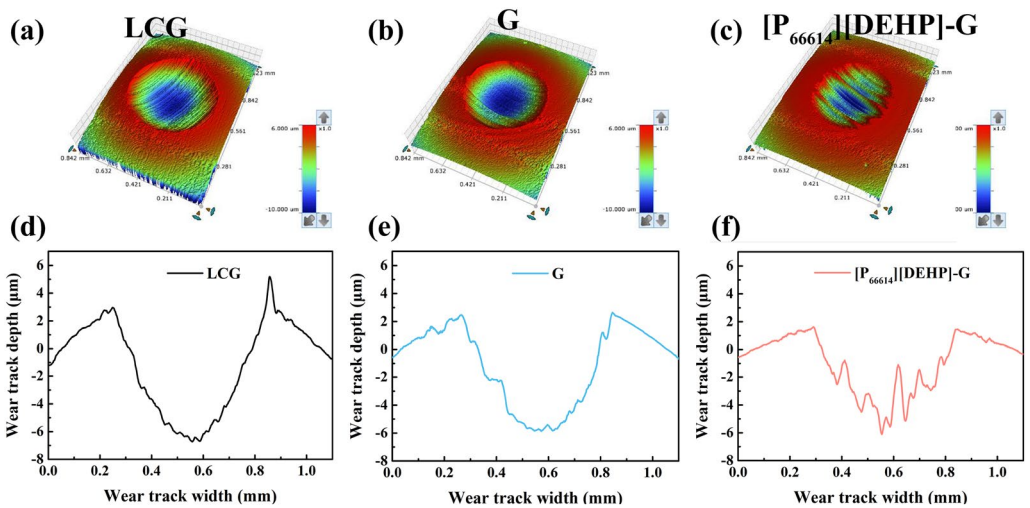

Figure 7 3D morphology and 2D wear profile of worn surfaces by (**a**, **d**) LCG, (**b**, **e**) G-LCG, (**c**, **f**) [P_{66614}][DEHP]-G-LCG at 490 N

morphology images of the worn surfaces. The worn surface of LCG is more severely abraded, with craters formed by spalling and deeper furrows, indicating severe abrasive and adhesive wear. In contrast, the worn surfaces of G-LCG and [P_{66614}][DEHP]-G-LCG exhibit lighter abrasive wear (Figures 8e and f) with relatively shallow and narrow plough grooves, which demonstrates that both G-LCG and [P_{66614}][DEHP]-G-LCG show excellent wear resistance. Additionally, the wear resistance of [P_{66614}][DEHP]-G-LCG is marginally superior to that of G-LCG. These results suggest that the anti-wear performance of LCG is improved by incorporating well-dispersed graphene.

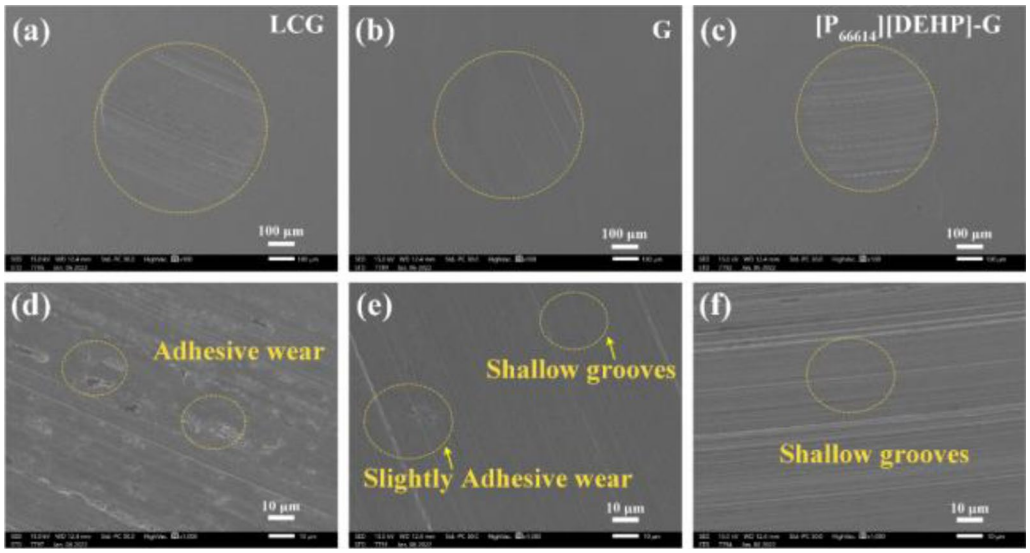

Figure 8 SEM images of worn surface lubrication with (**a**, **d**) LCG, (**b**, **e**) G-LCG, and (**c**, **f**) $[P_{66614}][DEHP]$-G-LCG at 490 N

3.4 Analysis of Friction Mechanism

In order to further explore the lubrication mechanism of graphene lithium complex grease and to reveal the density and distribution of the deposited graphene-film on the friction interface, the Raman signal of graphene is examined over large areas on the wear surface. Optical micrographs of worn surfaces are shown in Figures 9(a) and (d). Figures 9(b) and (e) are the Raman scans of the G peaks (intensity at 1600 cm^{-1}) on the worn surfaces of G-LCG and $[P_{66614}][DEHP]$-G-LCG, respectively. The dark blue area represents the weak Raman signal of graphene, indicating that graphene is not adsorbed in the friction area. From green to orange to dark red, the brighter the areas, the stronger the Raman signals from graphene. Furthermore, the dark red color represents areas containing the strongest graphene Raman signals, meaning that these areas are covered by deposited graphene-film. Three different typical positions are taken

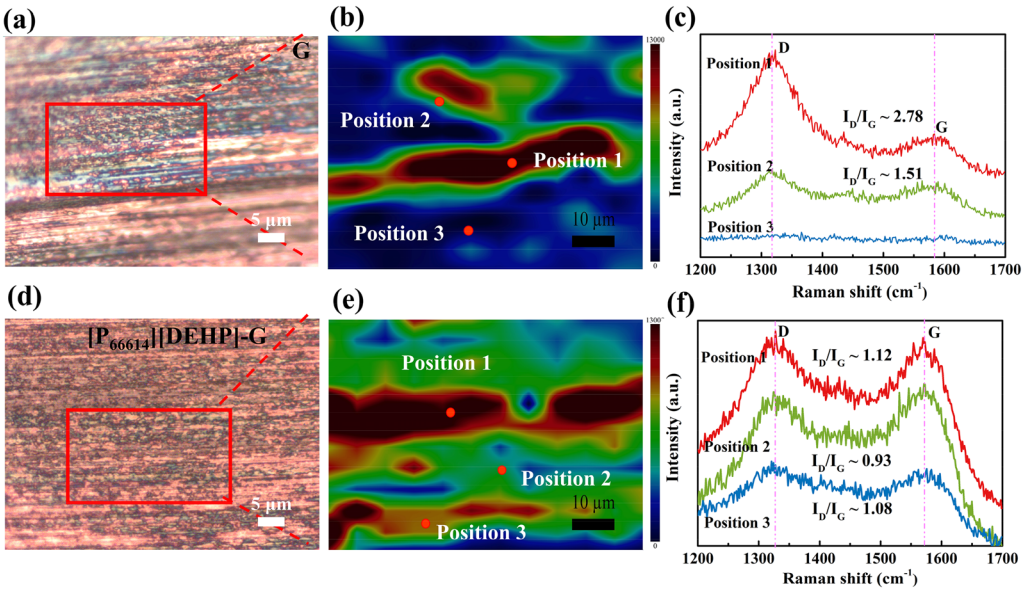

Figure 9 Optical microscope images, Raman mapping of the G band (intensity at 1600 cm^{-1}) and Raman spectra of three typical positions of the worn surface of steel balls after lubrication tests

from the Raman mapping scan of a worn surface. The corresponding Raman spectra are shown in Figures 9(c) and (f). The characteristic peaks G and D of graphene in G-LCG appear at position 1 (green) and position 2 (dark red), but not at position 3. However, [P_{66614}][DEHP]-G-LCG obviously has almost identical graphene Raman spectra at the three typical positions. The Raman results implied that deposited graphene-film is formed on the friction surface. In addition, the deposited graphene-film formed by [P_{66614}][DEHP]-G-LCG on the worn surface is denser and wider than that of G-LCG, primarily because of the higher dispersibility of modified-graphene in base oil. When the thickener fibers are squeezed, the base oil precipitates from the interlaced fiber skeleton during friction. Hence, graphene is likely to be absorbed on the friction interface with the precipitation of the base oil, forming a dense deposition graphene-film on the worn surface. Importantly, the I_D/I_G value of G and [P_{66614}][DEHP]-G after friction is larger than that before friction (in Figures 9(c) and (f)), showing that graphene is subjected to external force in the friction process, the interlayer slipped, the structure was destroyed, and new defects and disorders were formed and activated on the deposited graphene sheets [46]. The corresponding friction reduction and anti-wear effect of [P_{66614}][DEHP]-G-LCG are exhibited in Figures 5 and 6.

Here, the lubrication mechanisms of base grease and modified-graphene grease are shown in Figure 10. The oil molecules in grease are adsorbed on the metal surface to form an oil film, which is constantly destroyed during the friction process to form a new oil film [47, 48]. The presence of thickener fibers increased the thickness of oil film, and then oil film and thickener fibers acted together on the metal surface to form grease-film and tribo-chemical film [49]. More importantly, the formation of dense deposition graphene-film results in a decrease in the mutual contact of friction pairs, effectively avoiding friction between friction pairs and enabling their excellent lubricating properties. At the contact interface, the synergy of densely deposited graphene-film, spilled oil, and adhesive grease greatly enhances the lubrication function of grease.

4 Conclusions

In this study, three greases (LCG, G-LCG, and [P_{66614}][DEHP]-G-LCG) were successfully prepared. The physico-chemical and tribological properties were studied in detail, and the following conclusions can be drawn:

(1) As-prepared modified-graphene greases exhibit excellent physico-chemical properties, such as outstanding thermal stability, high dropping point over 230 °C, good corrosion resistance, low oil separation rates, and good colloidal stability.
(2) [P_{66614}][DEHP]-G-LCG exhibits excellent anti-friction properties (reducing by nearly 18.84%), and the wear volume lubricated by [P_{66614}][DEHP]-G-LCG is reduced by 67.34% compared to LCG.
(3) [P_{66614}][DEHP]-G-LCG has excellent lubrication functions and forms a denser and wider graphene deposition film on the friction interface. The excellent lubricity of modified-graphene lithium com-

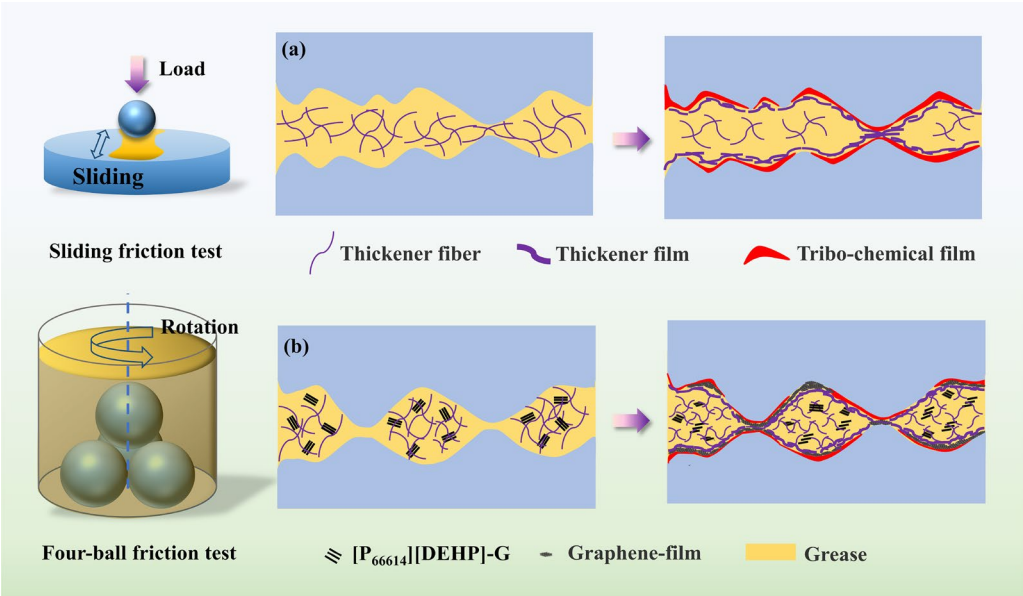

Figure 10 Schematic diagram of the lubricating mechanisms of (**a**) LCG and (**b**) [P_{66614}][DEHP]-G-LCG

plex grease is mainly attributed to the synergistic lubrication between the deposited graphene-film and grease film.

Acknowledgements
The authors gratefully acknowledge the Analytical and Testing Center of Southwest Jiaotong University for providing testing services.

Author contributions
XF and MZ developed the idea for this work; KL performed all measurements and characterization; ZZ, YL, ZZ, and XW analyzed and discussed the results, KL prepared the manuscript, XF reviewed and commented on the manuscript. All authors read and approved the final manuscript.

Authors' Information
Kaiyue Lin, born in 1997, is currently a postgraduate student at *School of Materials Science and Engineering, Southwest Jiaotong University, China*. Her major research interests include the performance characteristics of grease and the tribological properties of grease additives.
Zhuang Zhao, born in 1998, is a postgraduate student at *School of Materials Science and Engineering, Southwest Jiaotong University, China*. His research interests include the high dispersion of graphene additives in synthetic oils and their excellent tribological properties.
Yuting Li, born in 1996, is currently a doctoral candidate at *Southwest Jiaotong University, China*. Her research interests include the design of lubricating materials and the tribological properties of novel deep eutectic solvents.
Zihan Zeng, born in 1998, is currently a postgraduate student at *School of Materials Science and Engineering, Southwest Jiaotong University, China*. Her research interests include the tribological properties and mechanism of quantum dots as lubricating additives.
Xiaofeng Wei, born in 1998, is currently a master candidate at *School of Materials Science and Engineering, Southwest Jiaotong University, China*. He specializes in solid lubricating additives and functional thickener construction for enhancing the tribological properties of grease.
Xiaoqiang Fan, born in 1986, is currently a professor at *Southwest Jiaotong University, China*. His research focuses on lubricating materials, corrosion protection, and engineering applications.
Minhao Zhu, born in 1968, is currently a professor at *Southwest Jiaotong University, China*. His research areas cover fretting wear, fretting fatigue, surface engineering, and the design of fastener connections.

Funding
Supported by National Natural Science Foundation of China (Grant Nos. 52075458 and U2141211).

Data availability
Data will be made available on request.

Declarations

Competing Interests
The authors declare no competing financial interests.

Received: 8 November 2022 Revised: 21 September 2023 Accepted: 28 September 2023
Published online: 02 November 2023

References

[1] C L Lin, P A Meehan. Microstructure characterization of degraded grease in axle roller bearings. *Tribology Transactions*, 2019, 62(4): 667-687.
[2] I M Jamadar, D Vakharia. Correlation of base oil viscosity in grease with vibration severity of damaged rolling bearings. *Industrial Lubrication and Tribology*, 2018, 70(2): 264-272.
[3] S K Yeong, P F Luckham, T F Tadros. Steady flow and viscoelastic properties of lubricating grease containing various thickener concentrations. *Journal of Colloid and Interface Science*, 2004, 274(1): 285-293.
[4] P M Lugt. A review on grease lubrication in rolling bearings. *Tribology and Lubrication Technology*, 2010, 66(7): 44.
[5] C J Donahue. Lubricating grease: A chemical primer. *Journal of Chemical Education*, 2006, 83(6): 862-869.
[6] N Xu, X Wang, R Ma, et al. Insights into the rheological behaviors and tribological performances of lubricating grease: Entangled structure of a fiber thickener and functional groups of a base oil. *New Journal of Chemistry*, 2018, 42(2): 1484-1491.
[7] R Kreivaitis, J Padgurskas, M Gumbyte, et al. An assessment of beeswax as a thickener for environmentally friendly lubricating grease production. *Lubrication Science*, 2015, 27(6): 347-358.
[8] X Q Li, Y Y Yang, F Li. Comparative study on mechanical properties of sealing grease composed of different base oils for shield tunnel. *Materials*, 2020, 13(3): 692.
[9] N De Laurentis, P Cann, P M Lugt, et al. The influence of base oil properties on the friction behaviour of lithium greases in rolling/sliding concentrated contacts. *Tribology Letters*, 2017, 65(4): 128.
[10] C C Fang, X H Meng, X L Kong, et al. Transient tribo-dynamics analysis and friction loss evaluation of piston during cold and warm-start of a SI engine. *International Journal of Mechanical Sciences*, 2017, 133: 767-787.
[11] Y X Peng, X D Chang, S S Sun, et al. The friction and wear properties of steel wire rope sliding against itself under impact load. *Wear*, 2018, 400: 194-206.
[12] N F Garza Montes de Oca, W M Rainforth. Wear mechanisms experienced by a work roll grade high speed steel under different environmental conditions. *Wear*, 2009, 267(1-4): 441-448.
[13] J Y Zheng, L L Wu, J F Shi. Extreme pressure equipments. *Chinese Journal of Mechanical Engineering*, 2011, 24(2): 202-206.
[14] S S Rawat, A P Harsha, S Das, et al. Effect of CuO and ZnO nano-additives on the tribological performance of paraffin oil-based lithium grease. *Tribology Transactions*, 2020, 63(1): 90-100.
[15] B Zheng, J Zhou, X Jia, et al. Friction and wear property of lithium grease contained with copper oxide nanoparticles. *Applied Nanoscience*, 2020, 10: 1355-1367.
[16] H Chang, C W Lan, C H Chen, et al. Anti-wear and friction properties of nanoparticles as additives in the lithium grease. *International Journal of Precision Engineering and Manufacturing*, 2014, 15: 2059-2063.
[17] X B Ji, Y X Chen, G Q Zhao, et al. Tribological properties of CaCO3 nanoparticles as an additive in lithium grease. *Tribology Letters*, 2011, 41(1): 113-119.
[18] Q He, A Li, Y Guo, et al. Tribological properties of nanometer cerium oxide as additives in lithium grease. *Journal of Rare Earths*, 2018, 36(2): 209-214.
[19] A Saxena, D Kumar, N Tandon. Development of eco-friendly nano-greases based on vegetable oil: An exploration of the character via structure. *Industrial Crops and Products*, 2021, 172: 114033.
[20] Y Li, X Y Liu, D J Liu, et al. Surface Modified TiO_2 nanoparticles-an effective anti-wear and anti-friction additive for lubricating grease. *China Petroleum Processing and Petrochemical Technology*, 2017, 19(2): 74-79.
[21] B Jin, J Zhao, G Y Chen, et al. In situ synthesis of Mn_3O_4/graphene nanocomposite and its application as a lubrication additive at high temperatures. *Applied Surface Science*, 2021, 546: 149019.
[22] J Zhang, J T Li, A L Wang, et al. Improvement of the tribological properties of a lithium-based grease by addition of graphene. *Journal of Nanoscience and Nanotechnology*, 2018, 18(10): 7163-7169.
[23] C L Gan, T Liang, W Li, et al. Amine-terminated ionic liquid modified graphene oxide/copper nanocomposite toward efficient lubrication. *Applied Surface Science*, 2019, 491: 105-115.
[24] R Mehta, S Chugh, Z H Chen. Enhanced electrical and thermal conduction in graphene-encapsulated copper nanowires. *Nano Letters*, 2015, 15(3): 2024-2030.
[25] C Lee, X D Wei, J W Kysar, et al. Measurement of the elastic properties and intrinsic strength of monolayer graphene. *Science*, 2008, 321(5887): 385-388.
[26] K S Novoselov, A K Geim, S V Morozov, et al. Electric field effect in atomically thin carbon films. *Science*, 2004, 306(5696): 666-669.
[27] H D Wang, S Q Hu, K Takahashi, et al. Experimental study of thermal rectification in suspended monolayer graphene. *Nature Communications*, 2017, 8: 15843.

[28] Z J Li, Q He, S Du, et al. Effect of few layer graphene additive on the tribological properties of lithium grease. *Lubrication Science*, 2020, 32(7): 333-343.
[29] T C Ouyang, Y D Shen, R Yang, et al. 3D hierarchical porous graphene nanosheets as an efficient grease additive to reduce wear and friction under heavy-load conditions. *Tribology International*, 2020, 144: 106118.
[30] S S Rawat, A P Harsha, O P Khatri, et al. Pristine, reduced, and alkylated graphene oxide as additives to paraffin grease for enhancement of tribological properties. *Journal of Tribology*, 2021, 143(2): 021903.
[31] X P Li, C L Gan, Z Y Han, et al. High dispersivity and excellent tribological performance of titanate coupling agent modified graphene oxide in hydraulic oil. *Carbon*, 2020, 165: 238-250.
[32] H P Mungse, K Gupta, R Singh, et al. Alkylated graphene oxide and reduced graphene oxide: Grafting density, dispersion stability to enhancement of lubrication properties. *Journal of Colloid and Interface Science*, 2019, 541; 150-162.
[33] L Zhang, Y He, L Zhu, et al. Alkyl phosphate modified graphene oxide as friction and wear reduction additives in oil. *Journal of Materials Science*, 2019, 54(6): 4626-4636.
[34] A Mohammadi, M Hosseinipour, H Abdolvand, et al. Improvement in bioavailability of curcumin within the castor oil based polyurethane nanocomposite through its conjugation on the surface of graphene oxide nanosheets. *Polymers for Advanced Technologies*, 2022, 33(4): 1126-1136.
[35] A Chouhan, H P Mungse, O P Sharma, et al. Chemically functionalized graphene for lubricant applications: Microscopic and spectroscopic studies of contact interfaces to probe the role of graphene for enhanced tribo-performance. *Journal of Colloid and Interface Science*, 2018, 513: 666-676.
[36] S N Du, J L Sun, P Wu. Preparation, characterization and lubrication performances of graphene oxide-TiO_2 nanofluid in rolling strips. *Carbon*, 2018, 140: 338-351.
[37] C L Gan, T Liang, D L Chen, et al. Phosphonium-organophosphate modified graphene gel towards lubrication applications. *Tribology International*, 2020, 145: 106180.
[38] G L Ren, X W Sun, W Li, et al. Improving the lubrication and anti-corrosion performance of polyurea grease via ingredient optimization. *Friction*, 2021, 9(5): 1077-1097.
[39] M Fang, K G Wang, H B Lu, et al. Single-layer graphene nanosheets with controlled grafting of polymer chains. *Journal of Materials Chemistry*, 2010, 20(10): 1982-1992.
[40] P Solis Fernandez, J I Paredes, S Villar Rodil, et al. Determining the thickness of chemically modified graphenes by scanning probe microscopy. *Carbon*, 2010, 48(9): 2657-2660.
[41] J Lee, S Shin, S Kang, et al. Highly stable surface-enhanced Raman spectroscopy substrates using few-layer graphene on silver nanoparticles. *Journal of Nanomaterials*, 2015: 975043.
[42] Y W Zhu, S Murali, W W Cai, et al. Graphene and graphene oxide: synthesis, properties, and applications. *Advanced Materials*, 2010, 22(35): 3906-3924.
[43] C Chen, J B Xi, E Z Zhou, et al. Porous Graphene microflowers for high-performance microwave absorption. *Nano-Micro Letters*, 2018, 10(2): 26.
[44] B Lin, I Rustamov, L Zhang, et al. Graphene-reinforced lithium grease for antifriction and anti-wear. *ACS Applied Nano Materials*, 2020, 3(10): 10508-10521.
[45] S W Zhang, L T Hu, D Qiao, et al. Vacuum tribological performance of phosphonium-based ionic liquids as lubricants and lubricant additives of multialkylated cyclopentanes. *Tribology International*, 2013, 66: 289-295.
[46] J Zhao, J Y Mao, Y R Li, et al. Friction-induced nano-structural evolution of graphene as a lubrication additive. *Applied Surface Science*, 2018, 434: 21-27.
[47] M Niu, J Qu. Tribological properties of nano-graphite as an additive in mixed oil-based titanium complex grease. *RSC Advances*, 2018, 8(73): 42133-42144.
[48] L Huang, D Guo, X Liu, et al. Effects of nano thickener deposited film on the behaviour of starvation and replenishment of lubricating greases. *Friction*, 2016, 4(4): 313-323.
[49] F Cyriac, P M Lugt, R Bosman, et al. Effect of thickener particle geometry and concentration on the grease EHL film thickness at medium speeds. *Tribology Letters*, 2016, 61(2): 18.